Tunable, CW Laser Emission at 225 nm via Intracavity Frequency Tripling in a Semiconductor Disk Laser

Julio M. Rodríguez-García, David Pabœuf, and Jennifer E. Hastie, *Senior Member, IEEE*

***Abstract*—Numerous applications would benefit from a compact laser source with tunable, continuous-wave emission in the deep ultraviolet (wavelengths <250 nm); however, very few laser sources have been demonstrated with direct emission in this spectral region and options are generally limited to pulsed, fixed wavelength sources or complex and impractical setups for nonlinear frequency mixing of the emission of several infrared lasers in various external enhancement cavities. Here, we propose an all-solid-state, continuous-wave, tunable laser with emission between 224 and 226 nm via intracavity frequency tripling in an AlGaInP-based semiconductor disk laser (SDL). Output power up to 78 μW is achieved in continuous wave operation, with a tuning range over 350 cm^{-1}. AlGaInP-based SDLs may be designed to emit anywhere between ∼640–690 nm such that wavelengths between 213 and 230 nm may be targeted for specific applications using a similar set-up. An in-depth study of the nonlinear conversion has been carried out to understand the limitations of the set-up, namely large walk-off angles for phase-matching in the nonlinear crystals, and the potential for increasing the output power to several milli-Watts. This is, to the authors' knowledge, the first implementation of intracavity frequency tripling in a visible SDL and the shortest wavelength emitted from an SDL system.**

***Index Terms*—Semiconductor lasers, surface emitting lasers, ultraviolet sources, continuous wave, tunable, frequency conversion, harmonic generation, nonlinear optics.**

I. Introduction

INDUCING electronic transitions in small molecules, such as some organic compounds and reactive species containing nitrogen and oxygen, requires high energy photons, with energy >4.5 eV (deep ultraviolet light; UVC: 100 nm–280 nm) [1]–[4]. As a result, lasers in this spectral region are of considerable interest for spectroscopy; however, such lasers tend to operate in the pulsed regime (with the disadvantage of systematic frequency shifts [5]) and at fixed wavelengths. For example, direct emission at such short wavelengths can be achieved with excimer or gas lasers; in particular, HeAg lasers emit at 224.3 nm [6].

Nonlinear frequency conversion can be an efficient means to reach the UV region from more convenient and practical solid-state sources, although access to wavelengths <250 nm is limited by phase-matching requirements, absorption and walk-off effects on the material side, and of course by the fundamental spectral range of the laser source. Current technology for continuous wave (CW), UV generation is mostly based on frequency up-conversion in external resonators, since the high power stored in the resonator allows for efficient frequency conversion within the nonlinear crystal. While this method makes use of enhanced optical fields, it leads to rather complex and bulky setups, with further complexity if active stabilization is required. These set-ups can be simplified by removing the external resonator, although this reduces the conversion efficiency, and so several passes through the same nonlinear stage are often used [7]. While it is possible to obtain high conversion efficiency with a single nonlinear crystal, a multi-crystal scheme has advantages in terms of reduced walk-off with improved beam quality. In any case, with frequency up-conversion there is typically a compromise between continuous wave operation, tunability and high power.

Dye lasers are one of the few *tunable* ultraviolet laser sources, albeit with the inherent difficulties and drawbacks of working with non-solid-state gain media (e.g., cumbersome architecture, toxicity and high cost). Ti:Sapphire lasers are the most common all-solid state alternative for broad tuning, having shown emission throughout a wide range of wavelengths [8]–[10]; however, the lower limit of their fundamental spectral range means that higher harmonics are required to reach the deep UV and such systems are usually pulsed.

Previously reported CW, UVC laser systems include single frequency operation at 213 nm via sum frequency mixing (in an external enhancement cavity) of the outputs of an amplified 1064 nm Nd:YAG laser and an externally-quadrupled Nd:YVO_4 laser to reach the fifth harmonic [11], and the generation of over 2 mW at 194 nm via sum-frequency mixing of the amplified output of a 792 nm diode laser with the second harmonic of a 514 nm argon ion laser (frequency-doubled in an external enhancement cavity) [12]. Of particular note is the recent result by Ruhnke *et al.* of 16 μW CW at 222.5 nm via frequency

Manuscript received January 31, 2017; revised March 15, 2017; accepted April 16, 2017. This work was supported in part by the U.K. Engineering and Physical Sciences Research Council under Challenging Engineering Award EP/I02279/1. The work of J. M. Rodríguez-García was supported in part by the Fraunhofer Centre for Applied Photonics, Glasgow, U.K. *(Corresponding author: Julio M. Rodríguez-García.)*

J. M. Rodríguez-García and J. E. Hastie are with the Institute of Photonics, Department of Physics, University of Strathclyde, Technology & Innovation Centre, Glasgow G1 1RD, U.K. (e-mail: julio.rodriguez@strath.ac.uk; jennifer.hastie@strath.ac.uk).

D. Pabœuf was with the Institute of Photonics, University of Strathclyde, Glasgow G1 1RD, U.K. He is now with the M Squared Lasers Ltd., Glasgow G20 0SP, U.K (e-mail: david.paboeuf@m2lasers.com).

Color versions of one or more of the figures in this paper are available online at http://ieeexplore.ieee.org.

Digital Object Identifier 10.1109/JSTQE.2017.2696882

This work is licensed under a Creative Commons Attribution 3.0 License. For more information, see http://creativecommons.org/licenses/by/3.0/

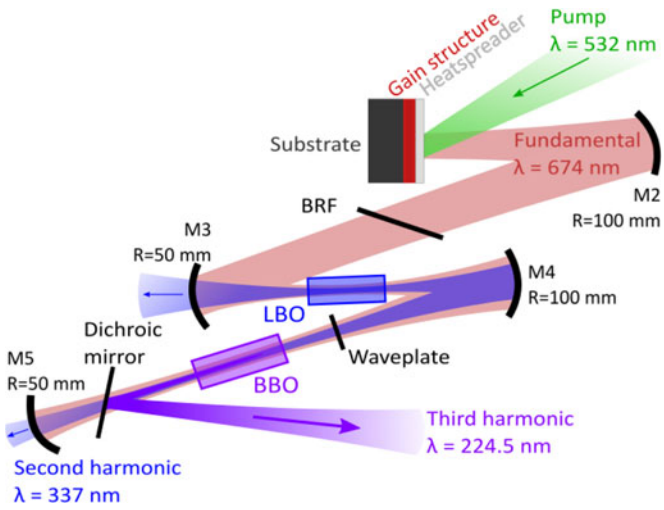

Fig. 1. Schematic diagram of the frequency-tripled SDL. BRF: birefringent filter; M2–M5: high reflectivity mirrors. The heatspreader is a 0.5mm-thick uncoated diamond window.

doubling of a high power, single frequency GaN external cavity diode laser [13].

In summary, there are two main issues to be addressed for many applications that require a deep UV laser source: complexity and the wavelengths that can be achieved with a CW system. In this paper we propose to use semiconductor disk laser technology to address both.

Semiconductor disk lasers (SDLs), also known as VECSELs [14], provide high power in continuous wave operation with good beam quality, narrow linewidth and tunable wavelength. One of the main advantages is that the gain medium can be wavelength-engineered whilst retaining the ability to operate with high spatial brightness: while the first SDLs worked at wavelengths around 1 μm, fundamental operation has since been demonstrated at a wide variety of wavelengths, from 640 nm to beyond 5 μm [15], [16], with pioneering demonstrations at wavelengths as short as 400 nm [17]. Single frequency UVC emission has previously been demonstrated by Kaneda *et al.* by obtaining multi-Watt operation from an infrared SDL and then achieving efficient second and fourth harmonic generation in successive external enhancement cavities [18], [19]. However, the external cavity of SDLs, and low optimum output coupling, typically on the order of a few percent, mean that the emitting wavelength range is often efficiently extended by means of *intracavity* nonlinear frequency conversion, i.e., without the requirement for additional external resonators [15], [20].

Here we report an AlGaInP-based SDL, frequency tripled via intracavity sum-frequency mixing of the fundamental wavelength with its second harmonic, with the resulting emission in the UVC region. This approach takes advantage of the aforementioned qualities of the SDLs, transferring them to the deep UV region, where laser options are very limited, while aiming for compactness and simplicity of the setup. Intracavity frequency tripling has been previously studied and tested for conversion from the infrared, mostly in pulsed Nd: lasers [21]–[24]. There is one demonstration of a tripled infrared SDL [25]; however, the wavelength achieved is in the near UV (355 nm) and a full analysis of the optimisation of the nonlinear conversion is not reported. For the experiment reported here the fundamental wavelength is in the visible, 674 nm, the second harmonic is at 337 nm and the third harmonic at 224.5 nm. The resulting emission is tunable over 350 cm^{-1}, with an output power of 78 μW. To our knowledge, this is the first implementation of intracavity frequency tripling in a visible SDL and the shortest wavelength emitted from an SDL to date.

We begin by presenting the experimental setup in Section II-A, including the cavity configuration and selection of nonlinear crystals. Results for the intracavity tripled SDL (power outputs, tuning range) are discussed in Section II-B. Section III-A focusses on understanding the limitations caused by non-collinear propagation of the intracavity beams and the overlap mismatch. Finally, the efficiency of the process is compared with predictions from the theory of nonlinear frequency conversion in Section III-B.

II. Experiment

A. Experimental Setup

Red-emitting SDLs are capable of Watt-level output power, typically using three mirror cavities with 2–3% output coupling (see e.g., [26], [27]). The intracavity power of such high finesse SDL cavities is on the order of several 10s of Watts. The SDL employed for this work has been shown to be capable of reaching 100 W intracavity power in a three mirror cavity configuration, while this power drops to 63 W and 25 W in SHG and SFG configurations respectively, due to the intracavity losses caused by the inclusion of the different optical elements, as described below.

The SDL gain structure is similar to the one described in [28], where further details can be found. Briefly, the gain region consists of ten pairs of 6-nm thick GaInP quantum wells separated by AlGaInP barriers and positioned for resonant periodic gain (one pair per field anti-node). This gain medium is grown over a distributed Bragg reflector (DBR), composed of 40 AlAs/AlGaAs $\lambda/4$ layers. The whole structure is grown on a GaAs substrate. The device is optically-pumped with a commercial, diode-pumped solid-state laser at 532 nm.

A 500-μm-thick diamond heatspreader is bonded onto the intracavity surface of the SDL for thermal management, and the whole structure is clamped in a water-cooled brass mount and pumped with up to 5.5 W at 532 nm. The heatsink temperature was maintained at 2 °C. The diamond is not anti-reflection (AR) coated, resulting in pump reflection loss of $\sim$18%. The pump beam is focused into the SDL to a spot of $\sim$43 μm radius, mode matched with the fundamental laser beam. The fundamental emission occurs at $\sim$674 nm so that deep UV emission at $\sim$224.5 nm can be achieved via tripling. The third harmonic generation (THG) process is divided in two nonlinear stages: Intracavity second harmonic generation (SHG) is used to produce a beam at $\sim$337 nm (UVA), which propagates nearly collinearly with the fundamental beam. The fundamental and the SHG beams are re-focused in a second nonlinear crystal for sum-frequency

TABLE I
CRYSTAL PROPERTIES

	Crystal	Phase-matching	d_{eff} (pm/V)	Walk-off (mrad)
SHG	LBO	Type-I	0.61	18.93
	BBO	Type-I	1.95	76.86
SFG	BBO	Type-I	1.55	82.60

Comparison of crystal properties for the SHG process (674 → 337) and the SFG process (674 + 337 → 224.5). Data extracted from SNLO (SNLO nonlinear optics code available from A. V. Smith, AS-Photonics, Albuquerque, NM).

generation (SFG), producing the third harmonic, as shown in Fig. 1.

Among the most common crystals suitable for SHG at 674 nm are β-barium borate (BBO) and lithium triborate (LBO). Both have high transmission in the visible and near UV, and while BBO benefits from a higher nonlinear coefficient, LBO offers a smaller walk-off angle (see Table I). A lower walk-off angle gives better collinearity between the fundamental and SHG beams, which means better overlap in the SFG crystal, and thus higher efficiency, as long as the nonlinear coefficient is still reasonable. For this reason we use LBO as the SHG crystal. Periodically-poled crystals could potentially provide a perfectly collinear second harmonic beam; however, at these short wavelengths, the current technology is limited to 3rd order quasi-phase-matching with short crystal lengths [29].

In this work, SHG is achieved in a 7mm-long LBO crystal; the length was chosen as a compromise between nonlinear conversion efficiency and walk-off effects (see Sections III-A and III-B). It is cut for type-I phase-matching of conversion of 674 nm to 337 nm ($\theta = 90°$, $\varphi = 47.3°$). The second harmonic beam is produced with extraordinary polarization (perpendicular to the fundamental polarization) and is nearly collinear with the fundamental beam: the separation at the exit of the crystal is calculated to be $\sim$40 μm (see Section III-A). Both faces of the crystal are anti-reflection coated for the fundamental and second harmonic wavelengths (R $< 0.1\%$).

The choice of SFG crystal is very limited due to absorption and difficulty of phase-matching at these wavelengths. BBO stands apart as the only widely available option. It has a fairly large nonlinear coefficient ($d_{\text{eff}} = 1.55$ pm/V); however, it suffers from a large walk-off angle (82.60 mrad) and from some absorption at 224.5 nm ($\alpha = 0.12$ cm^{-1}). SFG is achieved in a 5mm-long BBO crystal cut for type-I phase-matching for conversion of 674 nm and 337 nm to 224.5 nm ($\theta = 58.1°$). The fundamental and SHG beams are focused and overlapped in this crystal, achieving the conditions to produce third harmonic by SFG.

Since both of the nonlinear crystals are cut for type-I phase-matching, the polarization of the second harmonic, which emerges from the SHG crystal perpendicular to the fundamental, must be rotated before entering the SFG crystal. This is achieved via a dual waveplate placed between the crystals, acting as a full waveplate for the fundamental beam (leaving it unaffected) and as a half waveplate for the second harmonic beam (90° rotation). This intracavity element is antireflection coated for both the fundamental and the second harmonic wavelengths (R $< 0.4\%$ at 674 nm; R $< 1.5\%$ at 337 nm).

The 5-mirror cavity has been designed by means of the ABCD-matrix formalism to provide three beam waists, maximizing the efficiency of both frequency conversion steps (Fig. 1). The fundamental beam waist radii are calculated to be 43 μm at the SDL, 14 μm at the SHG crystal and 39 μm at the SFG crystal. All mirrors have high reflectivity at the fundamental wavelength (R $> 99.9\%$). Mirrors M_3 and M_5 have high transmission at 337 nm (T $> 98\%$), while M_4 is highly reflective at this wavelength (R $> 99\%$). The laser wavelength can be tuned by rotating a 4mm-thick quartz birefringent filter (BRF) positioned at Brewster's angle inside the cavity. The BRF also narrows the linewidth and forces the fundamental polarization to be horizontal.

To avoid UVC absorption in M_5, the 224.5 nm beam generated in the SFG crystal is reflected out of the cavity by a dichroic mirror, coated for high reflectivity at the third harmonic wavelength (R $> 99.9\%$). Its placement at Brewster's angle ensures high transmission for the fundamental beam, removing the need for AR coating at this wavelength.

B. Laser Characterization

We have carried out a preliminary characterization of the 5-mirror cavity for SHG, i.e., without the dual waveplate, the BBO crystal and the dichroic mirror (hereafter referred to as 'SHG setup') in order to provide a baseline for assessment of the third harmonic generation step. The only intracavity elements present in this case are the BRF and the 7 mm-long SHG crystal (LBO).

The intracavity fundamental power reaches 63 W and the total second harmonic power produced is >120 mW (>60 mW per beam) as shown in Fig. 2, SHG setup, resulting in a nonlinear conversion efficiency of 0.2% from intracavity fundamental power to the second harmonic. A nonlinear conversion efficiency of >0.5% in an AlGaInP-based VECSEL has previously been achieved using intracavity BBO [30], [31]; however, as explained at the beginning of this section, higher conversion by means of using BBO instead of LBO is not desirable in this particular experiment due to higher walk-off reducing the collinearity of the SHG beam with the fundamental. The measurement of the power transfer to the second harmonic for the SFG setup, also shown in Fig. 2, shows the effect of adding the intracavity elements needed for SFG (i.e., dual waveplate, BBO crystal and dichroic mirror) causing losses to the intracavity fundamental power, and therefore a drop in the generated SH. We estimate the total additional insertion losses at the fundamental wavelength to be $\sim$3%. The intracavity fundamental to SHG conversion efficiency remains just under 0.2%. The output SHG power measured for both beams did not differ by more than 1%.

With all elements included in the cavity, we are able to demonstrate third harmonic emission. Fig. 3 shows the ultraviolet emission spectrum of the laser for 4 W input power, measured using an Avantes CCD spectrometer with resolution 0.4 nm. Two peaks can be observed: the peak on the left, at 224.5 nm,

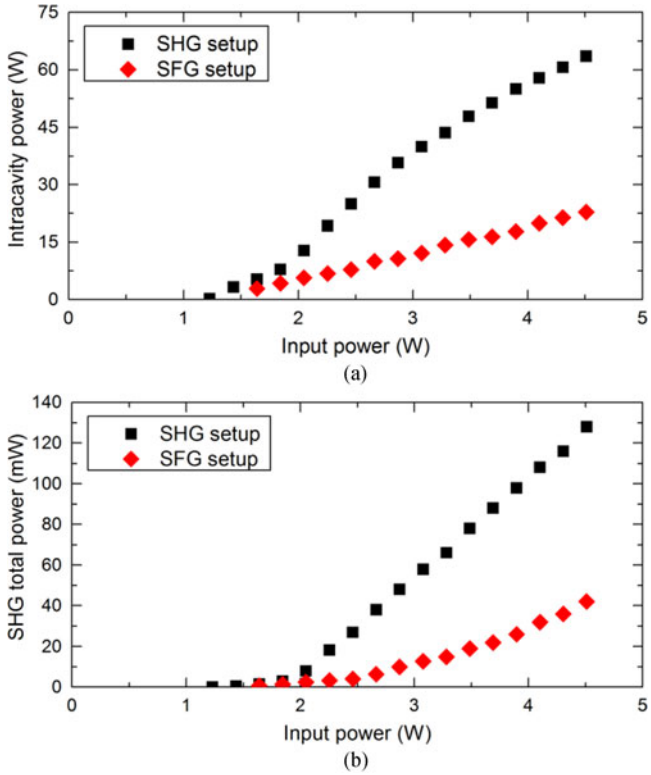

Fig. 2. (a) Intracavity power at the fundamental wavelength of 674 nm as a function of the input power. This intracavity power is deduced by measuring the leak through mirror M4, with measured transmission of 0.014% at 674 nm. (b) Total second harmonic power as a function of the input power. The two curves compare the performance of SHG between the cavity setup for SHG (black squares) and the cavity setup for SFG (red diamonds).

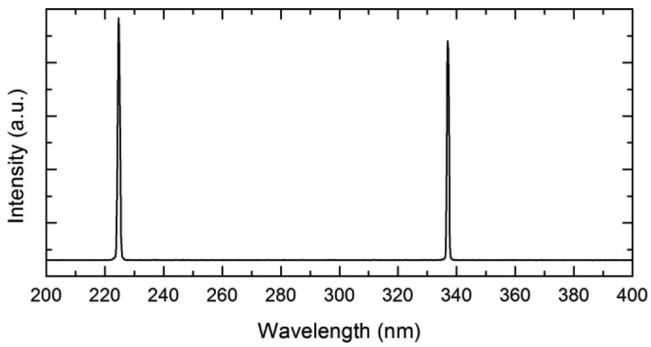

Fig. 3. UV region of the laser emission spectrum showing the second and third harmonics. The resolution of the spectrometer is 0.4 nm.

corresponds to the third harmonic of our fundamental wavelength; the peak on the right corresponds to the second harmonic beam, at 337 nm. The linewidth of the third harmonic peak is $\sim$1 nm.

By rotating the BRF and reorienting both nonlinear crystals to optimise phase-matching, the output wavelength of this laser can be tuned between 223.8 nm and 225.6 nm, as shown in Fig. 4 (inset). This corresponds to the fundamental wavelength tuning over 5.4 nm, which is less than the $>$10 nm tuning that may be achieved from this laser without nonlinear conversion.

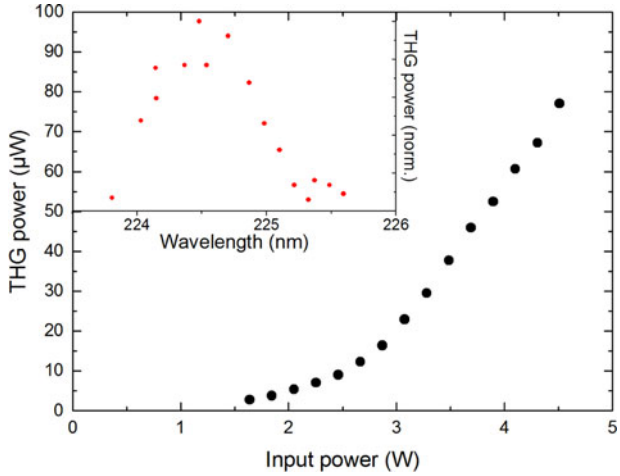

Fig. 4. Main: Third harmonic beam output power as a function of the pump power. Almost 78 μW of power is obtained at 224.5 nm. Inset: Normalised UVC output power of the laser as the wavelength is tuned by rotation of the birefringent filter. The tuning range is 350 cm^{-1}.

Nevertheless, 1.8 nm tuning in the UVC corresponds to a tuning range of 350 cm^{-1}, comparable with typical tuning ranges of SDLs at other wavelengths [30], [32]–[35].

With 4.5 W of input power, 78 μW output power is produced at the third harmonic, as shown in Fig. 4. The intracavity power of the fundamental is estimated to be around 26 W, while the power of the second harmonic is estimated to be around 30 mW per beam; in the current configuration only one of the generated second harmonic beams contributes to the SFG process (see Fig. 1). The threshold for the fundamental is around 1.1 W of pump power, but no THG can be detected below 1.6 W of pump. The efficiency of the second harmonic to third harmonic conversion is calculated to be 0.4%. This conversion efficiency is limited mainly by the divergence of the beams and by the walk-off induced by the nonlinear materials. We refer the reader to Sections III-A and III-B for detailed analysis.

In the following sections we will study the factors that limit the THG power in the current set-up, particularly the walk-off: Section III-A will deal with in-cavity beam propagation, and Section III-B will focus on the theoretical limits for SFG conversion.

III. Theoretical Study

A. Beam Propagation

Type-I critically phase-matched SHG produces a second harmonic beam with extraordinary polarization within the nonlinear crystal, and the Poynting vector of this beam is at an angle to the optical axis (walk-off). As a result, the SHG beam is separated from the fundamental beam at the exit of the crystal, with the separation determined by the length of the crystal. This separation is maintained, if not increased, as the beams propagate through the cavity and the reduced overlap between the fundamental and second harmonic beams will limit the efficiency of SFG. We therefore begin our analysis by calculating the distribution of both beams inside the SFG crystal.

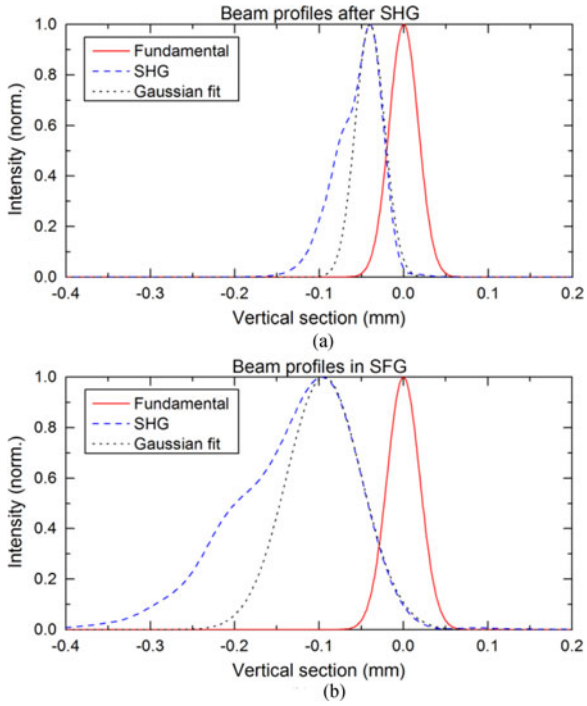

Fig. 5. (a) Beam profiles at the exit of SHG crystal. (b) Beam profiles inside the SFG crystal. A Gaussian profile has been fitted to the SHG beam, in order to define the beam size. The beam profiles correspond to the vertical section, which is the direction of effect of the walk-off. The zero corresponds to the optical axis of the cavity, on which the fundamental beam is centred.

The geometry of the fundamental beam is determined by the geometry of the laser cavity. As described in Section II-A, the fundamental beam has a waist of 14 μm radius at the SHG crystal and 39 μm radius at the SFG crystal. The beam parameters of the second harmonic generated in the SHG crystal can be obtained using Kleinman's equation for the SHG electric field at the exit of the nonlinear crystal (see equation 4.20 in [36]). This equation allows us to calculate the corresponding SHG profile for a given profile of the fundamental. The resulting beam profiles are plotted in Fig. 5(a). The maximum intensity of the SHG beam is located 40 μm away from the optical axis of the cavity, where the fundamental beam is centred. The effect of the walk-off on the beam shape is visible on the left side of this profile, which is wider and exhibits additional features. As seen in Fig. 5(a), at the exit of the crystal the fundamental beam size is 35 μm radius, while the beam size of a Gaussian fit of the SHG is 50 μm radius.

The two beams, fundamental and second harmonic, then travel through the cavity towards the second non-linear crystal, in which SFG is achieved. Propagation of both beams is modelled using the Fresnel diffraction formalism [37]. The first step consists of propagating the beams from the LBO crystal to the folding mirror M_4; done by computing the fast Fourier transform of each beam and using the propagator:

$$H(z,\sigma,\lambda) = \exp\left(i\frac{2\pi}{\lambda}z\sqrt{1-\lambda^2\sigma^2}\right) \tag{1}$$

where z is the propagation distance and σ the spatial frequency in the Fourier domain. The wavelength is defined as $\lambda = \lambda_0/n$ to take into account the optical index of the medium. The focussing effect of the curved mirror is taken into account by applying a spherical phase:

$$T(x,\lambda) = \exp\left(\frac{i\pi x^2}{\lambda R/2}\right) \tag{2}$$

where R is the radius of the mirror (mirror M_4 in our case). The final step consists of re-applying (1) in the Fourier domain to propagate the beams to (and through) the second non-linear crystal.

The resulting beam profiles at the centre of the SFG crystal are plotted in Fig. 5(b). It can be seen that the distance between the intensity peaks has increased from 40 μm to 95 μm. The fundamental beam waist is 35 μm radius, in agreement with the values obtained by the ABCD-matrix formalism. The SHG beam profile becomes further stretched with propagation through the cavity; however, a Gaussian fit shows that the side overlapping the fundamental remains close to a Gaussian profile, as can be seen in Fig. 5(b). In order to define an upper limit to the expected conversion, we will consider the Gaussian fit of the SHG for the SFG theory detailed in the following section. The beam waist radius of this Gaussian fit is 90 μm, and it contains almost 70% of the total SHG power. Given the separation between the peaks, very tight focusing would decrease the beam overlap, while loose focusing would not provide the high intensities required for nonlinear interaction. The set-up used experimentally is a compromise between these two considerations.

B. SFG Efficiency

BBO offers a high nonlinear coefficient for the SFG process, which is unfortunately compromised by the large walk-off angle present at our phase-matching wavelengths (Table I). This walk-off inherently affects the conversion efficiency of the process, severely limiting the output power. Boyd and Kleinman modelled this behaviour by means of a so called h function, which modifies the output power (neglecting pump depletion) [38]:

$$P_3 = \frac{32\pi^2 d_{\mathrm{eff}}^2}{\varepsilon_0 c n_3^2 \lambda_1\lambda_2\lambda_3} P_1 P_2 e^{-\alpha L} L \cdot h(B,\xi) \tag{3}$$

In the equation P_3 is the output (THG) power, while P_1 and P_2 correspond to the input fundamental intracavity power and SHG power. Crystal length (L), crystal nonlinear coefficient $(\mathrm{d}_{\mathrm{eff}})$, crystal absorption coefficient (α), crystal refractive index at THG wavelength (n_3) and all three wavelengths are also present.

This h function shows that the process heavily depends on a focusing parameter $\xi = L/b$, with $b = 2z_0$ being the confocal parameter and L the length of the crystal; and on a birefringent, or walk-off, parameter B proportional to the walk-off angle ρ, the wavenumber and the length of the crystal:

$$\mathrm{B} = \rho/2\sqrt{\mathrm{L}(\mathrm{k}_1+\mathrm{k}_2)/2} \tag{4}$$

Boyd and Kleinman's study showed that larger values of the walk-off parameter correspond to smaller values of the h function, and hence lower output power. At the same time the

TABLE II
EXPERIMENTAL PARAMETERS

λ_ω	$\lambda_{2\omega}$	w_ω^0	$w_{2\omega}^0$
674 nm	337 nm	39 μm	90 μm
P_ω	$P_{2\omega}$	L	d_{eff}
26 $\pm$ 4 W	30 $\pm$ 5 mW	5 mm	1.55 pm/V
n_ω	$n_{2\omega}$	$n_{3\omega}$	ρ
1.665	1.712	1.696	82.60 mrad

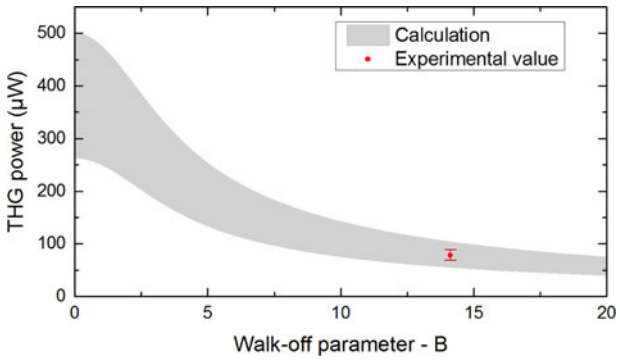

Fig. 6. Effect of walk-off parameter in the SFG process, calculated using the parameters in Table II. B = 14 is the walk-off parameter value in our experiment.

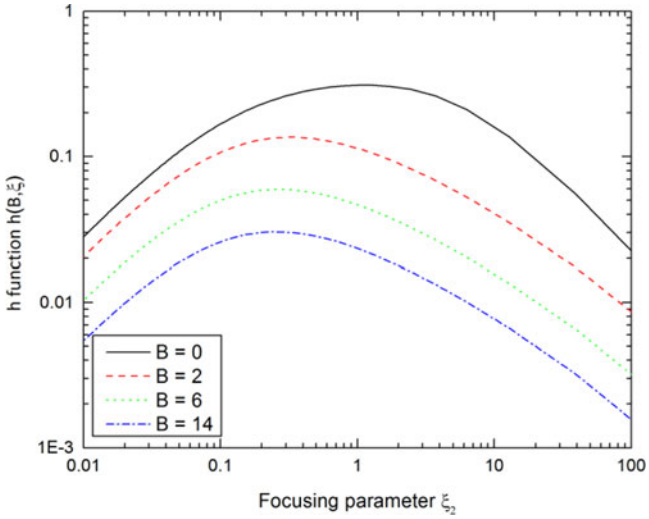

Fig. 7. h function vs the SHG focusing parameter ξ_2 for different B parameter values. For our experimental conditions ($B = 14$), the walk-off effect reduces the output power by an order of magnitude with respect to the case of no walk-off.

optimum focusing condition changes towards weaker focussing as the walk-off increases.

Guha and Falk generalized Boyd and Kleinman's study by considering mixing of Gaussian beams with different confocal parameters [39]. As mentioned in Section II-A, the parameters of the fundamental beam are defined by the geometry of the cavity (beam waist of 39 μm in the SFG crystal). While the previous calculations have shown that the SHG beam was off-centre and not Gaussian, we define an upper limit on the likely conversion by now considering it to be Gaussian and coaxial with the fundamental, with a diameter of 90 μm, which corresponds to the size of the Gaussian fit on Fig. 5(b). According to the theory, the efficiency of SFG conversion is strongly dependent on the beam sizes, but also on the nonlinear coefficient and the walk-off angle.

We computed Guha and Falk's generalized h function (equation 39 in [39]) numerically for our experimental parameters, summarized in Table II. We assume $\Delta k = 0$ for all calculations (see Appendix).

The walk-off angle for a given crystal is fixed by the phase-matching angle at the desired wavelengths. In the case of this study, the wavelengths 674, 337 and 224.5 nm have phase-matching at $\theta = 58.1°$ in BBO, with a corresponding walk-off angle of 82.60 mrad. If the crystal is 5-mm-long, the corresponding walk-off parameter is $B = 14$. The calculated output power is limited to approximately a hundred μW for our experimental conditions. In Fig. 6 we have plotted the results for the expected output power of the SFG process as a function of the walk-off parameter, to show its impact on the conversion efficiency. The total output power is relatively sensitive to small variations in the input powers (P_ω and $P_{2\omega}$), and therefore we have plotted an upper and lower limit to the THG power estimation to account for the error introduced by small uncertainty in the transmission of the HR mirrors through which the low power fundamental and second harmonic beams were detected. It can be seen that the maximum output power rapidly decreases from around half a mW to the hundred μW level as the walk-off parameter increases to our experimental value. This shows that, for the given input power, the third harmonic power achieved in this experiment was as good as could be expected given the walk-off of BBO. As a comparison, in the more common process 1064 nm + 532 nm $\rightarrow$ 355 nm the required phase-matching orientation corresponds to a walk-off parameter of $B = 10$ in BBO, while it would be $B = 2.4$ in LBO (which offers phase matching at these wavelengths). The corresponding h function would be respectively 2 and 5 times larger than in our case and therefore higher conversion would be expected.

Fig. 7 shows the dependence of the h function with the focusing parameter of the SHG beam for different walk-off parameters. The optimum value of the h function tends towards looser focusing for larger B values (that is to say walk-off suppresses the conversion more strongly for tighter focussing).

A means to reduce the impact of walk-off, the use of several pieces of the nonlinear crystal (either separated in space or built in a monolithic structure), has been extensively studied by Zondy *et al.* [40]–[42]. With this technique, the walk-off directions in two consecutive sections of the crystal are opposite to each other, and therefore compensate one another. Walk-off compensated (WOC) structures have already been used experimentally to demonstrate improved SHG [43]. In our particular experiment, they would provide the extra advantage of removing the walk-off-induced separation between the fundamental and second harmonic beams, making them collinear throughout the cavity.

A monolithic WOC structure has a lower walk-off parameter B for equivalent crystal length. As an example, if we were to

use a monolithic structure made of five 1-mm-thick plates with a total length of 5 mm (same length as our BBO crystal) for our SFG process, the walk-off parameter would be $B = 6$, as opposed to the current value of $B = 14$ (curves plotted in Fig. 7), and roughly doubling the output power (see Fig. 6).

For our experiment, use of WOC-BBO structures as nonlinear crystals for both SHG and SFG processes would offer higher SHG powers with better overlap between the SFG input beams and, furthermore, increased efficiency of the SFG for substantial improvement of the THG output power. However monolithic WOC structures are not widely available commercially and such improvements remain the subject of future work.

IV. Conclusion

We have demonstrated third harmonic generation in a visible SDL, providing continuous wave laser emission in the deep ultraviolet region of the electromagnetic spectrum and producing the shortest wavelength to date from an SDL. The laser generates emission of 78 μW continuous wave at 224.5 nm, with a tuning range over 350 cm^{-1}. Compared with other schemes used to achieve CW, UVC laser emission (e.g., [8], [9]), the setup is relatively compact thanks to the short fundamental wavelength (requiring fewer conversion steps) and the fact that the frequency conversion is carried out intracavity.

We have studied the limitations to the output power of our current nonlinear conversion set-up, and shown that the second to third harmonic conversion achieved is as high as could be expected given the large value of the walk-off angle for the corresponding phase-matching in BBO. The use of walk-off compensating structures or periodically-poled crystals would allow significant improvements to the conversion efficiency, subject to commercial availability at the wavelengths of interest.

AlGaInP-based SDLs are a relatively immature laser technology and improvements to their efficiency are still being made with further optimisation of the gain structure (see e.g., multi-Watt CW operation recently reported by Mateo *et al.* [31]), such that the fundamental power available for conversion can be significantly increased. We therefore expect that tunable, deep UV output on the order of several mW could be generated using this type of laser. Further, SDLs based on this material have shown fundamental emission from 640 nm–690 nm such that wavelengths between approximately 213 nm–230 nm may be targeted for specific applications, including, but not limited to, two-photon absorption of atomic oxygen and xenon [3], vibrational bands of NO, O_2 [44], metal transitions [45], etc. Such a compact, solid-state laser solution offers many advantages over the few alternatives available at wavelengths <230 nm, thus opening up new applications and the opportunity to make others more practical for use outside the laboratory.

Appendix

Since the optimal phase-matching value is not necessarily $\Delta k = 0$ (see [38] for discussion), we have calculated the variation of h with phase mismatch $\Delta k{\cdot}L$ for two different conditions: for our experimental walk-off $(B = 14)$ and focusing; and in absence of walk-off $(B = 0)$ with tighter focusing. The results are plotted in Fig. 8, and confirm that in our case no phase mismatch is desired. While the experimental work is not heavily affected by this result (since the crystal is manually aligned to the maximizing position), we assume $\Delta k = 0$ for all calculations.

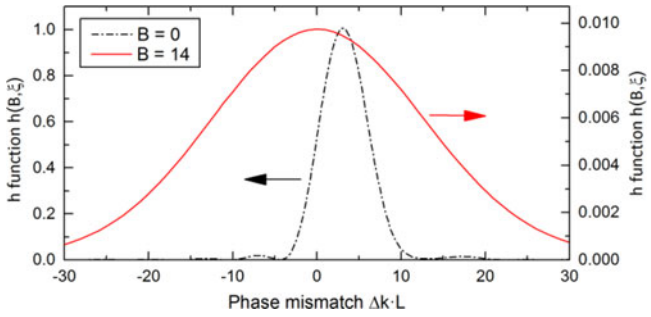

Fig. 8. Effect of phase-matching in the SFG process. For B = 14 curve the peak is centred at $\Delta k = 0$. For B = 0 curve the optimum phase-matching value is greater than 0.

Acknowledgment

The semiconductor gain structure wafer was grown by A. B. Krysa at the EPSRC National Centre for III-V Semiconductors, University of Sheffield, U.K.

Dataset: Data related to this publication have been made available at the University of Strathclyde data repository. https://dx.doi.org/10.15129/dc8f4692-d009-4a27-9cf4-fb9f2b9381f9

References

[1] C. Schulz, V. Sick, J. Heinze, and W. Stricker, "Laser-induced-fluorescence detection of nitric oxide in high-pressure flames with A–X (0, 2) excitation," *Appl. Opt.*, vol. 36, no. 15, pp. 3227–3232, May 1997.

[2] J. Amorim, G. Baravian, and J. Jolly, "Laser-induced resonance fluorescence as a diagnostic technique in non-thermal equilibrium plasmas," *J. Phys. D. Appl. Phys.*, vol. 33, no. 9, pp. R51–R65, May 2000.

[3] K. Niemi, V. S. der Gathen, and H. F. Döbele, "Absolute calibration of atomic density measurements by laser-induced fluorescence spectroscopy with two-photon excitation," *J. Phys. D. Appl. Phys.*, vol. 34, no. 15, pp. 2330–2335, Aug. 2001.

[4] C. Bonnin *et al.*, "224 nm deep-UV laser for native fluorescence, a new opportunity for biomolecules detection," *J. Chromatography A*, vol. 1156, no. 1/2, pp. 94–100, 2007.

[5] S. Galtier, F. Nez, L. Julien, and F. Biraben, "Ultraviolet continuous-wave laser source at 205 nm for hydrogen spectroscopy," *Opt. Commun.*, vol. 324, pp. 34–37, Aug. 2014.

[6] M. C. Storrie-Lombardi, W. F. Hug, G. D. McDonald, A. I. Tsapin, and K. H. Nealson, "Hollow cathode ion lasers for deep ultraviolet Raman spectroscopy and fluorescence imaging," *Rev. Sci. Instrum.*, vol. 72, no. 12, pp. 4452–4459, Dec. 2001.

[7] K. Devi, S. Parsa, and M. Ebrahim-Zadeh, "Continuous-wave, single-pass, single-frequency second-harmonic-generation at 266 nm based on birefringent-multicrystal scheme," *Opt. Express*, vol. 24, no. 8, pp. 8763–8775, 2016.

[8] S. Sayama and M. Ohtsu, "Tunable UV CW generation by frequency tripling of a Ti:sapphire laser," *Opt. Commun.*, vol. 137, no. 4–6, pp. 295–298, May 1997.

[9] X. Zhang *et al.*, "Widely tunable and high-average-power fourth-harmonic generation of a Ti:sapphire laser with a KBBOF prism-coupled device," *Opt. Lett.*, vol. 34, no. 9, pp. 1342–1344, May 2009.

[10] F. Huang, Q. Lou, T. Yu, J. Dong, B. Lei, and Y. Wei, "Tunable solid state UV laser," *Opt. Laser Technol.*, vol. 33, no. 2, pp. 111–115, Mar. 2001.

[11] J. Sakuma, Y. Asakawa, T. Sumiyoshi, and H. Sekita, "High-Power CW Deep-UV coherent light sources around 200 nm based on external resonant sum-frequency mixing," *IEEE J. Sel. Topics Quantum Electron.*, vol. 10, no. 6, pp. 1244–1251, Nov. 2004.
[12] D. J. Berkeland, F. C. Cruz, and J. C. Bergquist, "Sum-frequency generation of continuous-wave light at 194 nm," *Appl. Opt.*, vol. 36, no. 18, pp. 4159–4162, Jun. 1997.
[13] N. Ruhnke *et al.*, "Single-pass UV generation at 222.5 nm based on high-power GaN external cavity diode laser," *Opt. Lett.*, vol. 40, no. 9, pp. 2127–2129, May 2015.
[14] M. Kuznetsov, F. Hakimi, R. Sprague, and A. Mooradian, "Design and characteristics of high-power (>0.5-W CW) diode-pumped vertical-external-cavity surface-emitting semiconductor lasers with circular TEM00 beams," *IEEE J. Sel. Topics Quantum Electron.*, vol. 5, no. 3, pp. 561–573, May/Jun. 1999.
[15] S. Calvez, J. E. Hastie, M. Guina, O. G. Okhotnikov, and M. D. Dawson, "Semiconductor disk lasers for the generation of visible and ultraviolet radiation," *Laser Photon. Rev*., vol. 3, no. 5, pp. 407–434, Sep. 2009.
[16] N. Schulz, J.-M. Hopkins, M. Rattunde, D. Burns, and J. Wagner, "High-brightness long-wavelength semiconductor disk lasers," *Laser Photon. Rev*., vol. 2, no. 3, pp. 160–181, Jul. 2008.
[17] R. Debusmann *et al.*, "InGaN-GaN disk laser for blue-violet emission wavelengths," *IEEE Photon. Technol. Lett.*, vol. 22, no. 9, pp. 652–654, May 2010.
[18] Y. Kaneda *et al.*, "Continuous-wave all-solid-state 244 nm deep-ultraviolet laser source by fourth-harmonic generation of an optically pumped semiconductor laser using CLBO in an external resonator," *Opt. Lett.*, vol. 33, no. 15, pp. 1705–1707, Aug. 2008.
[19] Y. Kaneda *et al.*, "Continuous-wave, single-frequency 229 nm laser source for laser cooling of cadmium atoms," *Opt. Lett.*, vol. 41, no. 4, pp. 705–708, Feb. 2016.
[20] A. Rahimi-Iman, "Recent advances in VECSELs," *J. Opt.*, vol. 18, no. 9, Sep. 2016, Art. no. 93003.
[21] R. S. Craxton, "Theory of high efficiency third harmonic generation of high power Nd-glass laser radiation," *Opt. Commun.*, vol. 34, no. 3, pp. 474–478, Sep. 1980.
[22] R. Wu, "High-efficiency and compact blue source: Intracavity frequency tripling by using LBO and BBO without the influence of birefringence," *Appl. Opt.*, vol. 32, no. 6, pp. 971–975, Feb. 1993.
[23] Z. Sun *et al.*, "Generation of 4.3-W coherent blue light by frequency-tripling of a side-pumped Nd:YAG laser in LBO crystals," *Opt. Express*, vol. 12, no. 26, pp. 6428–6433, Dec. 2004.
[24] B.-T. Zhang *et al.*, "Generation of 7.8W at 355 nm from an efficient and compact intracavity frequency-tripled Nd:YAG laser," *Opt. Commun.*, vol. 283, no. 11, pp. 2369–2372, Jun. 2010.
[25] Q. Shu *et al.*, "Intracavity-tripled optically-pumped semiconductor laser at 355 nm," vol. 7193, 2009, Art. no. 719319.
[26] J. E. Hastie *et al.*, "Tunable ultraviolet output from an intracavity frequency-doubled red vertical-external-cavity surface-emitting laser," *Appl. Phys. Lett.*, vol. 89, no. 6, Aug. 2006, Art. no. 61114.
[27] T. Schwarzbäck *et al.*, "Short wavelength red-emitting AlGaInP-VECSEL exceeds 1.2 W continuous-wave output power," *Appl. Phys. B*, vol. 102, no. 4, pp. 789–794, Mar. 2011.
[28] J. E. Hastie *et al.*, "High power CW red VECSEL with linearly polarized TEM00 output beam," *Opt. Express*, vol. 13, no. 1, pp. 77–81, Jan. 2005.
[29] J. Hirohashi *et al.*, "300 mW 355 nm generation by PP-LBGO," *Adv. Solid State Lasers*, vol. 1, 2014, Paper ATu4A.4.
[30] H. Kahle *et al.*, "High optical output power in the UVA range of a frequency-doubled, strain-compensated AlGaInP-VECSEL," *Appl. Phys. Express*, vol. 7, no. 9, Sep. 2014, Art. no. 92705.
[31] C. M. N. Mateo *et al.*, "Efficiency and power scaling of in-well and multi-pass pumped AlGaInP VECSELs," *Proc. SPIE*, vol. 9734, 2016, Art. no. 973410.
[32] J. E. Hastie *et al.*, "0.5-W single transverse-mode operation of an 850-nm diode-pumped surface-emitting semiconductor laser," *IEEE Photon. Technol. Lett.*, vol. 15, no. 7, pp. 894–896, Jul. 2003.
[33] J. Paajaste *et al.*, "High-power and broadly tunable GaSb-based optically pumped VECSELs emitting near 2μm," *J. Cryst. Growth*, vol. 311, no. 7, pp. 1917–1919, Mar. 2009.
[34] L. Fan *et al.*, "Highly strained InGaAsGaAs multiwatt vertical-external-cavity surface-emitting laser emitting around 1170 nm," *Appl. Phys. Lett.*, vol. 91, no. 13, pp. 2005–2008, 2007.
[35] R. Abram, K. Gardner, E. Riis, and A. Ferguson, "Narrow linewidth operation of a tunable optically pumped semiconductor laser.," *Opt. Express*, vol. 12, no. 22, pp. 5434–5439, 2004.
[36] D. A. Kleinman, A. Ashkin, and G. D. Boyd, "Second-harmonic generation of light by focused laser beams," *Phys. Rev.*, vol. 145, no. 1, pp. 338–379, May 1966.
[37] J. W. Goodman, *Introduction to Fourier optics*, 3rd ed. Engleweood, CO, USA: Roberts & Company Publishers, 2005.
[38] G. D. Boyd and D. A. Kleinman, "Parametric interaction of focused gaussian light beams," *J. Appl. Phys.*, vol. 39, no. 8, 1968, Art. no. 3597.
[39] S. Guha and J. Falk, "The effects of focusing in the three-frequency parametric upconverter," *J. Appl. Phys.*, vol. 51, no. 1, pp. 50–60, Jan. 1980.
[40] J.-J. Zondy, "Comparative theory of walkoff-limited type-II versus type-I second harmonic generation with Gaussian beams," *Opt. Commun.*, vol. 81, no. 6, pp. 427–440, Mar. 1991.
[41] J.-J. Zondy, C. Bonnin, and D. Lupinski, "Second-harmonic generation with monolithic walk-off-compensating periodic structures. I. Theory," *J. Opt. Soc. Amer. B*, vol. 20, no. 8, pp. 1675–1694, Aug. 2003.
[42] J.-J. Zondy, D. Kolker, C. Bonnin, and D. Lupinski, "Second-harmonic generation with monolithic walk-off-compensating periodic structures. II. Experiments," *J. Opt. Soc. Amer. B*, vol. 20, no. 8, pp. 1695–1707, Aug. 2003.
[43] K. Hara, S. Matsumoto, T. Onda, W. Nagashima, and I. Shoji, "Efficient ultraviolet second-harmonic generation from a walk-off-compensating bBBO device with a new structure fabricated by room-temperature bonding," *Appl. Phys. Express*, vol. 5, no. 5, May 2012, Art. no. 52201.
[44] I. J. Wysong, J. B. Jeffries, and D. R. Crosley, "Laser-induced fluorescence of O, O2, and NO near 226 nm: photolytic interferences and simultaneous excitation in flames," *Opt. Lett.*, vol. 14, no. 15, pp. 767–769, Aug. 1989.
[45] W. S. Fann, R. Storz, H. W. K. Tom, and J. Bokor, "Direct measurement of nonequilibrium electron-energy distributions in subpicosecond laser-heated gold films," *Phys. Rev. Lett.*, vol. 68, no. 18, pp. 2834–2837, May 1992.

Julio M. Rodríguez-García received the Lic.es Sci. degree in physics from Universidad Autónoma of Madrid, Madrid, Spain, in 2013. He is currently working toward the Ph.D. degree at the University of Strathclyde, Glasgow, U.K., on the topic of CW, ultraviolet semiconductor disk lasers.

David Pabœuf received the Ingénieur degree from Ecole Supérieure d'Optique, Palaiseau, France, in 2006, the M.Sc. degree in optics and photonics in 2006, and the Ph.D. degree in physics from the Université Paris Sud, Orsay, France, in 2009, where he worked on the coherent combination of laser diodes. From 2012 to 2016, he was a Research Associate in the Institute of Photonics, University of Strathclyde and is currently in M Squared Lasers Ltd. His main research interests include the field of narrow-linewidth solid-state lasers including optical parametric oscillators and vertical external cavity surface emitting lasers.

Jennifer E. Hastie (SM'12) received the B.Sc. degree in laser physics and optoelectronics in 2000 and the Ph.D. degree in 2004 in physics from the University of Strathclyde, Glasgow, U.K., where she studied vertical external cavity surface emitting lasers.

She is currently a Reader in the Institute of Photonics, Department of Physics, University of Strathclyde, Technology & Innovation Centre. Her main research interests include the area of optically-pumped semiconductor disk lasers for high spatial and spectral brightness and broad tunability in the ultraviolet, visible, and infrared. Her current topics include continuous wave, tunable solid-state Raman lasers, including diamond Raman lasers, and narrow linewidth lasers at novel wavelengths for quantum technology applications including optical clock systems. She is a senior member of the Optical Society of America.